Check for updates

Gelation and luminescence of lanthanide hydrogels formed with deuterium oxide†

Yusuke Zama,[a] Kazushige Yanai,[b] Juri Takeshita,[b] Ayumi Ishii,[acde] Masamichi Yamanaka [ID] *[be] and Miki Hasegawa [ID] *[ae]

Gel formations and efficient lanthanide luminescence appeared in deuterium oxide (D$_2$O) medium instead of light water (H$_2$O), and their solvation possibilities by using luminescence lifetimes were discussed. The lanthanide ions in the hydrogel of **1** obtained by H$_2$O (abbreviated as H$_2$O-Ln**1**; Ln = Eu, Tb, and Gd) in our previous report act as the coupling part between neighbor molecules for the bundle structure. Here, D$_2$O also acts as a medium to form the lanthanide-hydrogel of **1**, and increases intensities of luminescence for Tb, because a soft crystalline state reducing resonance thermal relaxation is realized. The gel-formation and luminescence band positions of Ln**1** in D$_2$O corresponded to those in H$_2$O. From the observation of luminescence lifetimes in H$_2$O and D$_2$O, the number of coordinating water molecules on Eu and Tb were estimated to be around 3 or 4 for both. The luminescence intensity of Eu**1** did not increase even in D$_2$O, due to a blue shift of the excited triplet state of **1**, as compared to that in H$_2$O.

Introduction

Deuterium oxide is a key matrix to induce ff-emission regarding trivalent lanthanide (abbreviated to Ln) complexes.[1–5] For instance, Bruce *et al.* cordially explained the influence of the vibrational mode of a hydrogen/deuterium–oxygen for the enhancement or quenching of luminescence of Ln^{3+} such as Tb^{3+} and Eu^{3+} in their coordination compounds. The ff-emissions of Ln^{3+} are sensitized by the antenna effect by the coordination of π-electronic systems with high absorption coefficient. Lanthanide luminescent materials have recently attracted considerable attention, due to their brightness and sharp bands.[1–4] For instance, trivalent Tb in a complex exhibits green emission, which originates from ff transitions that have no influence on any organic ligands because they exist independently in the core of the atom.[5] Organic ligands act as photo-antennas to provide the excitation energy to the central metal. Additionally, the luminescence intensities of Tb complexes show temperature dependence, due to reverse energy transfer.[6]

The combination of two hetero Ln ions such as Tb and Eu with organic components can accomplish colour mixing of luminescence, and induce inter-metal energy transfer from Tb to Eu by UV excitation of the ligand moiety.[7–9] Such a stepwise energy transfer is also useful for developing luminescent sensors or devices. Recently, we reported mixed Tb/Eu systems in chain-structured complexes consisting of helical Ln complexes (abbreviated as LnL; Ln = Eu or Tb) linked by analogues of 1,4-benzenedicarboxylate (abbreviated as bdc).[10] The initial compound LnL-bdc showed no inter-metal energy transfer between the energy donor (ligand) and acceptor (centre metal ion), whereas bdc substituted with NH$_2$– or OH– induced inter-metal energy transfer in the chain complexes, and resulted in reddish-orange emission even with a 1 : 1 mixture of EuL and TbL, due to its amorphous structure.

It was reported that the intensity change of lanthanide luminescence is affected by O–H/O–D or C–H/C–D vibrational mode, due to harmonic resonance with the luminescent level in lanthanide ions.[11,12] It is known that the quenching mechanism for trivalent Eu and Tb involves resonance of the third and fourth overtones of O–H vibrations (*ca.* 3400 cm^{-1}) in H$_2$O, respectively.[13–15] We recently reported the effect of deuterium on the luminescent components of H/D-phenanthroline complexes with Eu, Tb, and Tm complexes, according to the appearance of polymorphism detected by the synchrotron X-ray powder diffraction (XRPD).[13]

A water-soluble lanthanide complex of helicate structure with π-electronic systems and two carboxyl groups, LnL^{COOH} also showed the change in luminescent intensity, when using D$_2$O instead of H$_2$O.[16] LnL^{COOH} retains its molecular and spectral stability in a wide pH range of 2.6–9.7.

^{a}*College of Science and Engineering, Aoyama Gakuin University, 5-10-1 Fuchinobe, Chuo-ku, Sagamihara, Kanagawa 252-5258, Japan. E-mail: haesmiki@chem. aoyama.ac.jp; Fax: +81-42-759-6221*

^{b}*Department of Chemistry, Faculty of Science, Shizuoka University, 836 Ohya, Suruga-ku, Shizuoka 422-8529, Japan. E-mail: yamanaka.masamichi@shizuoka.ac.jp*

^{c}*JST, PRESTO, 4-1-8 Honcho, Kawaguchi, Saitama, 332-0012, Japan*

^{d}*Graduate School of Engineering, Toin University of Yokohama, Kurogane-cho, Aoba-ku, Yokohama, Kanagawa 225-8503, Japan*

^{e}*Mirai Molecular Material Design Institute, Aoyama Gakuin Universitiy, 5-10-1 Fuchinobe, Chuo-ku, Sagamihara, Kanagawa 252-5258, Japan*

† Electronic supplementary information (ESI) available: Excitation and luminescence spectra and luminescence decay profiles. See DOI: 10.1039/c8ra08504h

To overcome the quenching problem related to Tb or Eu in H_2O, some investigators reported using a capsulated molecular structure to prohibit solvent molecules from reaching Ln ions.[17,18] A Ln complex (Ln = Eu, Tb, Dy, and Sm) with a 2-hydroxyisophthalamide derivative with a multidentate ligand has water solubility, and shows a 60% luminescence quantum yield for Ln = Tb, even in water.[17] Cluster-type Zn complexes with Ln $[Zn_8(ad)_4(BPDC)_6O \cdot 2Me_2NH_2, 8DMF, 11H_2O]$ (ad = adeninate; BPDC = biphenyldicarboxylate; DMF = dimethylformamide) form the metal–organic frameworks and show Ln luminescence even in water.[18]

Supramolecular gels, which are formed by self-assembly of small molecules, have attracted interest in recent decades because of their wide applicability.[19,20] Some luminescent lanthanide complexes in organogels and hydrogels have been developed and reported for applications such as paintable luminescent thermo sensors and color tunable LED fibers.[21–28] We also recently succeeded in obtaining bright luminescent Tb complexes with tris-urea-based hydrogelator **1** in H_2O.[29] The gelator shown in Fig. 1 has multiple roles in hydrogel formation, by coordinating with cations such as protons, divalent calcium, trivalent Ln ions, and serving as a photo-antenna to transfer excitation energy to Ln ions. Compound **1** also shows Ln selectivity in luminescence; the hydrogel of the lanthanide complex with **1** obtained with H_2O (abbreviated as H_2O-Ln**1**; Ln = Eu, Tb, and Gd) shows different luminescence quantum yields based on the Ln; for H_2O-Eu**1** and H_2O-Tb**1**, the quantum yields are <0.1% and 5.4%, respectively. It was recently revealed that the abovementioned lanthanide-including hydrogels of **1** act as media for organic fluorophores such as Rhodamine 6G,[30] and the interaction between the gelator and fluorophore was clearly enhanced in the luminescence as well as its lifetime.

Heavy water (D_2O) has been considered to be nearly equivalent to light water (H_2O), due to its physical properties in supramolecular hydrogels. Therefore, nuclear magnetic resonance (NMR) and small-angle neutron scattering (SANS) experiments have been performed in D_2O as an alternative to H_2O.[31] The similarities and dissimilarities of D_2O and H_2O are still unclear, and more study is required to clarify them. Here, we report a heavy water effect in the luminescence of a series of D_2O-Ln**1** based on measurements of electronic absorption, excitation, and luminescence spectra. Furthermore, the inter-metal energy transfer between Eu and Tb was induced in D_2O-Ln**1**. The luminescence lifetime and quantum yield were also measured to evaluate the luminescence efficiency in these hydrogels with Ln.

Results and discussion

Hydrogel formation and structure of D_2O-Ln1

Viscoelastic features of hydrogels D_2O-Ln1 and H_2O-Ln1. The viscoelastic properties of the hydrogels D_2O-Tb**1** and H_2O-Tb**1** were measured using a rheometer. The concentrations of **1** and $Tb(OTf)_3$ in hydrogels were fixed at 10 mM and 30 mM, respectively. The hydrogels D_2O-Tb**1** and H_2O-Tb**1** showed similar linear viscoelastic frequency sweep responses (Fig. 2a). Both the storage modulus (G') and the loss modulus (G'') were almost independent of the frequency from 0.1 to 10 rad s^{-1}. For both samples, G' was about twelve times larger than G''. The G' values for the hydrogels D_2O-Tb**1** and H_2O-Tb**1** at 1.0 rad s^{-1} were 42.8 and 42.7 kPa, respectively. Previously, we reported that the G' value for H_2O-Tb**1** at 1.0 rad s^{-1} was 8.1 kPa.[29] This result was obtained by measuring a relatively large hydrogel using a flat plate geometry (25 mm). Several pieces of the hydrogel were present in the measured sample. In the present study, we prepared the hydrogel in an aluminium cup (14 mm diameter) as a single continuous sample.[30] This unbroken sample exhibited a larger G' value. As shown in Fig. 2b, strain amplitude sweeps of D_2O-Tb**1** and H_2O-Tb**1** demonstrated elastic responses. The linear viscoelastic region of D_2O-Tb**1** was extensive, in comparison to that of H_2O-Tb**1**.

SEM and EDX measurement of hydrogels of Tb/Eu1. Energy dispersive X-ray (EDX) spectroscopy of the xerogel produced from a 1 : 1 mixture of hydrogels containing Eu**1** and Tb**1** is shown in Fig. 3. The peaks for Eu and Tb appear at 1.15 and 1.25 keV, respectively. The component ratios of elements are C, 73.8%; N, 9.8%; O, 13.8%; Tb, 1.9%; and Eu, 1.7%. Tb and Eu are localized on the fiber in equal amounts, which is consistent with the results of a previous study.[29]

Luminescence properties of D_2O-Ln1

Luminescence spectra of D_2O-Tb1 and D_2O-Eu1. D_2O-Tb**1**, a gel complex with trivalent Tb ions, was obtained as a hydrogel. Under UV light, the luminescence was a greenish colour to the naked eye. Electronic absorption spectra of D_2O-Ln**1** (Ln = Tb,
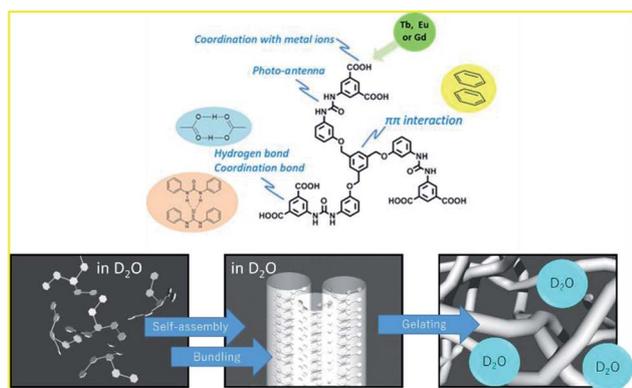

Fig. 1 Role of substances of **1** in the metal gelation (top), and schematic representation of gel formation in D_2O (bottom).
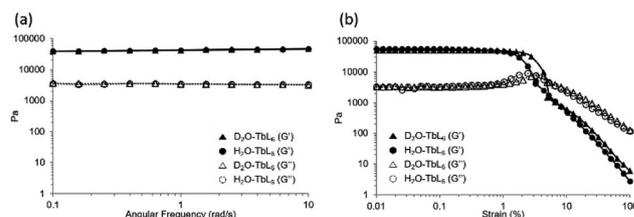

Fig. 2 G' and G'' values for D_2O-Tb**1** (triangles) and H_2O-Tb**1** (circles) (a) with a frequency sweep; (b) with a strain sweep.

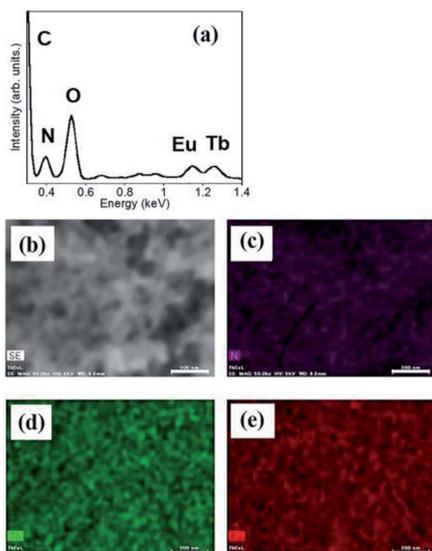Fig. 3 EDX spectrum (a), SEM image (b), and element maps ((c) N; (d) Tb and (e) Eu) of the xerogel obtained from hydrogels by mixing of **Eu1** and **Tb1**. Scale bar shows 100 μm.

Eu, and Gd) were measured (Fig. 4) to compare the electronic properties with those found previously for H_2O-**Ln1**. The bands at 288 and 323 nm and their shapes for D_2O-**Ln1** correspond well to those for H_2O-**Ln1**, meaning that their π-electronic states with D_2O completely matched those with H_2O. Additionally, the D_2O hydrogel of **1** without metal also shows the corresponding absorption band. This means that these metallo-hydrogels have similar π-electronic structures.

Luminescence spectra of D_2O-**Tb1** and D_2O-**Eu1** are shown in Fig. 5. D_2O-**Tb1** shows sharp luminescence bands at 489, 544, 583, and 621 nm assigned to the $^5D_4 \rightarrow {}^7F_6$, $^5D_4 \rightarrow {}^7F_5$, $^5D_4 \rightarrow {}^7F_4$, and $^5D_4 \rightarrow {}^7F_3$ transitions, respectively. The excitation spectra monitored at these luminescence band positions correspond to those for the electronic absorption spectra (Fig. S1†). Luminescence and excitation bands for D_2O-**Tb1** reproduced those of H_2O-**Tb1**, indicating that gelator **1** coordinates to the Ln ions while maintaining a suitable distance, to induce excitation energy transfer even in D_2O-**Tb1**.
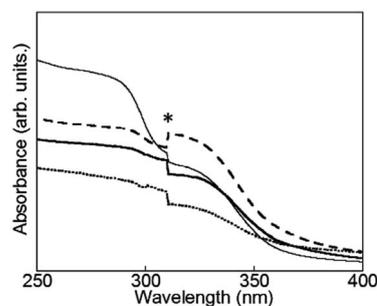

Fig. 4 Electronic absorption spectra of D_2O-**Tb1** (solid line), D_2O-**Eu1** (dotted line), D_2O-**Gd1** (dashed line), and D_2O-**H1** (thin line). * Due to apparatus.
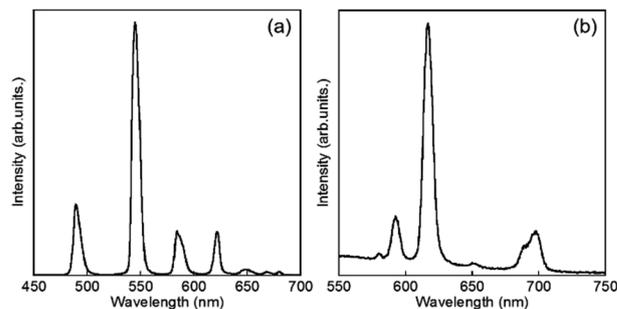
Fig. 5 Luminescence spectra of D_2O-**Tb1** (a) and D_2O-**Eu1** (b). λ_{ex} = 323 nm.

To evaluate the luminescence of D_2O-**Tb1** quantitatively, luminescence quantum yields and lifetimes were measured and are summarized in Table 1. From the luminescence decay curves monitored at 545 nm for both D_2O-**Tb1** and H_2O-**Tb1** (Fig. 6), it is clear that the luminescence decay for Tb in D_2O-**Tb1** was much slower than that for H_2O-**Tb1**. This indicates that the luminescence rate is influenced by the vibrational mode of the water medium. Based on the decomposition of the decay curves, D_2O-**Tb1** has at least three luminescent components, whereas the corresponding components in H_2O-**Tb1** were shorter than those in D_2O-**Tb1**. Surprisingly, the longest luminescence lifetime was for D_2O-**Tb1**. A typical value in terbium complexes in the solid state is *ca.* 1.5–1.7 ms. Thus, deuterium oxide accelerates Tb luminescence efficiently in the gel of D_2O-**Tb1**, and this is known as the heavy water effect. The luminescence quantum yield for D_2O-**Tb1** is twice that for H_2O-**Tb1**, which also supports the above conclusion. Thus, heavy water acts as an accelerator for Tb luminescence even in hydrogels.

D_2O-**Eu1** also exhibits luminescence bands at 580, 592, 616, 650, and 697 nm, which are assigned to the $^5D_0 \rightarrow {}^7F_0$, $^5D_0 \rightarrow {}^7F_1$, $^5D_0 \rightarrow {}^7F_2$, $^5D_0 \rightarrow {}^7F_3$, and $^5D_0 \rightarrow {}^7F_4$ transitions, respectively. These band positions are mostly the same for H_2O-**Eu1** (Fig. S2†). The luminescence quantum yields for Eu in D_2O-**Eu1** and H_2O-**Eu1** are quite low (Table 1). The luminescence decay profile for D_2O-**Eu1** was divided into two components, whose lifetimes are longer than those of H_2O-**Eu1**. This is in contrast to the two gel complexes with Tb, and may be also due to the vibrational mode of water as the medium.

The number of coordinating water molecules on Ln ions in hydrogels can be estimated using the experimental Horrocks' equation for the lifetime:[32–35]

Table 1 Luminescence quantum yields and lifetimes for D_2O-**Tb1** and D_2O-**Eu1** compared to those with light water[28]

	Quantum yields	Lifetimes/ms (amp); λ_{ex} = 340 nm[c]		
		τ_1	τ_2	τ_3
D_2O-**Tb1**	10%[a]	0.20(14%)	0.83(41%)	1.7(45%)
H_2O-**Tb1**	5.4%[a]	0.08(8%)	0.37(37%)	0.70(54%)
D_2O-**Eu1**	<0.1%[b]	0.32(25%)	1.06(75%)	—
H_2O-**Eu1**	<0.1%[b]	0.10(23%)	0.22(77%)	—

[a] λ_{obs} = 450–700 nm. [b] λ_{obs} = 550–750 nm. [c] λ_{mon} = 545 and 616 nm for Tb and Eu, respectively.
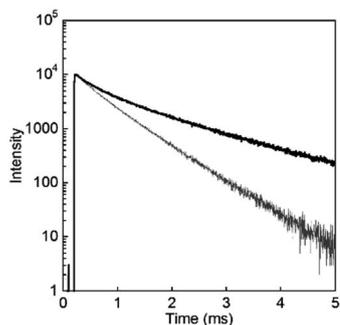
Fig. 6 Luminescence decay profiles for D_2O-Tb**1** (solid line) and H_2O-Tb**1** (thin grey line). λ_{mon} = 545 nm and λ_{ex} = 323 nm.

$$q^{Ln} = x(1/\tau_{H_2O} - 1/\tau_{D_2O}) \qquad (1)$$

where, q^{Ln} is the number of water molecules coordinating to a Ln ion, x is a fixed number (1.02 for Eu and 4.2 for Tb), and τ_{H_2O} and τ_{D_2O} are the average luminescence lifetimes (eqn (2)) observed in H_2O and D_2O, respectively:[36]

$$\tau = (a_1\tau_1^2 + a_2\tau_2^2)/(a_1\tau_1 + a_2\tau_2) \qquad (2)$$

Here, τ_n and a_n are the nth observed luminescence lifetime and its amplitude, respectively. We used the values in Table 1, and q_{Tb} and q_{Eu} were calculated as 3.7 and 3.1, respectively. Both metal ions in hydrogels will bind three or four water molecules. Thus, the O–H or O–D vibrational mode will directly affect the energy transfer efficiency or excitation energy relaxation, including non-radiative processes in these hydrogels.

To clarify the energy relaxation process for the water vibrational mode, ligand-centred emissions such as fluorescence and phosphorescence were observed. Fig. 7 shows fluorescence spectra of D_2O-H**1** and phosphorescence spectra of D_2O-Gd**1**. The compounds D_2O-H**1** and D_2O-Tb**1** also formed stable hydrogels similar to D_2O-Tb**1**. The use of Gd ion instead of a luminescent Ln ion is the conventional means for the determination of the singlet and triplet states as the energy donor in the π-electron system.[37] In our previous report, the fluorescence and phosphorescence bands for **1** using the hydrogel H_2O-Gd**1** were at 363 and 465 nm, respectively.[29] The corresponding bands appear at 363 (27 500 cm^{-1}) and 477 (21 000 cm^{-1}) nm,

respectively, in the present compounds. The 477 band acts as an energy donor to Tb or Eu in hydrogels. The phosphorescence band position for D_2O-Gd**1** is lower than that for H_2O-Gd**1** by 12 nm, and may affect the energy transfer efficiency of D_2O-Eu**1** which has acceptor bands around 394 or 416 nm.[38] Additionally, H_2O-Tb**1** and D_2O-Tb**1** show broad luminescence bands in laser Raman spectra at 637 (15 700 cm^{-1}) and 625 (16 000 cm^{-1}) nm, respectively (Fig. 8). These bands do not correspond to the fluorescence and phosphorescence in Fig. 6, suggesting that the luminescence bands are caused by strong intermolecular interactions by the formation of supramolecular hydrogels. It is noteworthy that the band position for self-assemblies of the gelator covers the Eu luminescence bands. In other words, the O–D vibrational mode intensified the luminescence of Tb in D_2O-Tb**1**. In contrast, the weakened luminescence for Eu in D_2O-Eu**1** was caused by the O–D vibration in deuterium oxide and by superimposition of the emission of self-assembly in the gelator and luminescence of Eu.

Luminescence spectra of D_2O-Tb/Eu1. Metal-to-metal excitation energy transfer between Tb and Eu suggests metal–metal interaction, by the measurement of their luminescence. We prepared the 1 : 1 mixed hydrogels of Eu and Tb with **1** in H_2O and D_2O, abbreviated as H_2O-Tb/Eu**1** and D_2O-Tb/Eu**1**, respectively. From the EDX measurement as described above, nitrogen in **1** was also found at the similar position with the metal ions. This supports luminescence effects such as inter-metal interactions between Tb and Eu in the mixed hydrogel of Eu**1** and Tb**1**.

Fig. 9 shows luminescence spectra of hydrogels containing Tb and Eu ions in a 1 : 1 ratio, which are abbreviated as H_2O-Tb/Eu**1** and D_2O-Tb/Eu**1** for light and heavy water, respectively. Bands at 544, 545, 584, 585, 620, 650(sh), and 679(sh) nm, assigned to the overlap of ff transitions of Tb^{3+} and Eu^{3+}, are observed for H_2O-Tb/Eu**1**. The corresponding bands for D_2O-Tb/Eu**1** appear at 544, 584, 590, 615, 649, and 696 nm, respectively.

The luminescence decay profile of H_2O-Tb/Eu**1** was monitored at both the emission band positions of Tb and Eu (Fig. S3† and Table 2). The decay curve of H_2O-Tb/Eu**1** monitored at 545 nm for Tb was divided into three luminescent components, and that at 616 nm for Eu into two. In the luminescence decay profile monitored at 616 nm for H_2O-Tb/Eu**1**, the luminescence rise curve for Eu was obtained and resulted in the time as 0.15 ms because the time range corresponds to the decay time of
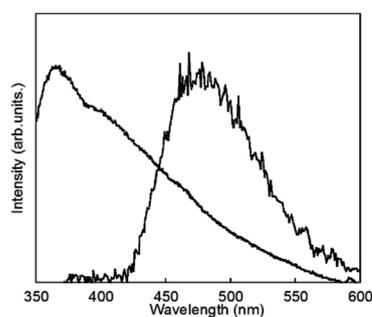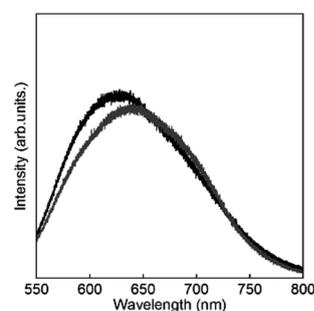

Fig. 7 Fluorescence spectrum of D_2O-H**1** (shorter wavelength band and phosphorescence spectrum at 77 K) and of D_2O-Gd**1** (longer wavelength band) localized on **1** (λ_{ex} = 323 nm).

Fig. 8 Luminescence spectra of D_2O-Tb**1** (black line) and H_2O-Tb**1** (grey line) observed by Raman spectroscopy (λ_{ex} = 532 nm).
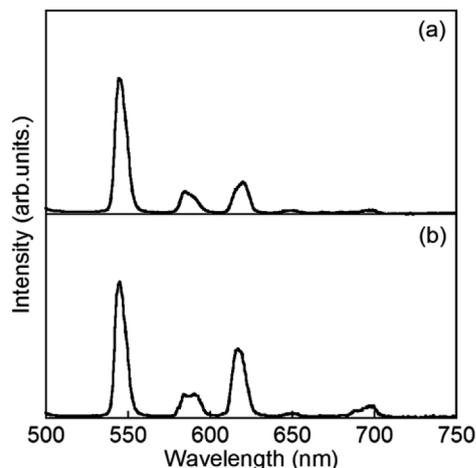
Fig. 9 Luminescence spectra of H_2O-Tb/Eu**1** and D_2O-Tb/Eu**1** (λ_{ex} = 323 nm).

0.19 ms for Tb. These results are consistent with Tb^{3+} ions transferring the excitation energy to Eu^{3+} in the mixed metal hydrogels. It also demonstrated that Tb and Eu would exist sufficiently close together, so as to promote metal-to-metal energy transfer in gels.[39] Similar metal-to-metal energy transfer was also observed in the xerogel obtained from hydrogels with both Tb and Eu. It should note to worth that the number of luminescent decay component of Eu in D_2O-Tb/Eu**1** is one; however, the rise in luminescence lifetime of 0.29 ms is higher than that in H_2O-Tb/Eu**1**. It suggests that the metal-to-metal energy transfer from Tb to Eu in the gel with D_2O is more efficient than that with H_2O.

The total luminescence quantum yield of Tb/Eu**1** was observed in the Tb and Eu emission region (500–750 nm). The quantum yield of D_2O-Tb/Eu**1** was 2%, which is higher than that of H_2O-Tb/Eu**1** and xerogel (<0.1%). These trends support the above discussion.

The xerogel obtained from hydrogels of Tb/Eu**1** showed the luminescence spectra and quantitative properties similar to those of the initial compound. It is also consistent that heavy water in this hydrogel system plays a role in enhancing lanthanide luminescence and inter-metal energy transfer. The increase in the φ value for the xerogel at 77 K means the increase in forwarded energy transfer from **1** to the Tb ion, because of the existence of thermal equilibrium between the donor and accepter levels in the Tb complexes.[7,9,40]

The energy diagram for Tb/Eu**1** systems is shown in Fig. 10. The excited triplet state of **1** acts as an energy donor to the terbium with less contribution of backward energy transfer.[29] However, the energy difference between **1** and the Eu ion is not suitable for efficient energy transfer. The mixing of Tb and Eu in the hydrogel formed with D_2O accomplished acceleration of Eu emission by Tb, through metal–metal energy transfer in D_2O-Tb/Eu**1**.

Experimental

Sample preparation

The gelator **1** and the gel containing Ln ions and D_2O were prepared as given in the previous paper using H_2O.[29,30] Lanthanide-containing hydrogels were obtained from light water and D_2O (Isotech Inc.), and lanthanide nitrates were used as the sources of metal ions (Ln = Eu, Tb and Gd). The 1 : 1 mixed hydrogels using Eu and Tb were also obtained by the mixing of europium nitrate and terbium nitrate equivalently. To obtain a metal-free hydrogel, hydrochloride and D_2O were used.

Apparatus

Rheological measurements were carried out on a DHR-2 rheometer (TA Instruments), using a flat plate geometry (8 mm). Electronic absorption and luminescence spectra were
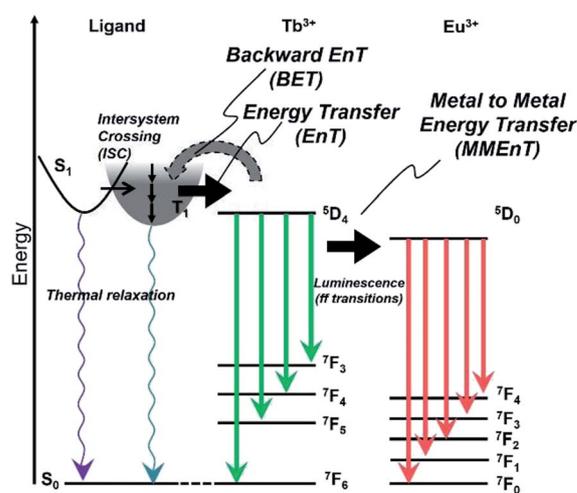

Fig. 10 Schematic representation of energy diagram for **1** and Tb-sensitizing of the Eu luminescence in hydrogels.

Table 2 Photophysical properties of mixed-metal systems in hydro/xerogels. λ_{ex} = 340 nm[d]

	Quantum yield[a]	Lifetimes/ms (amp.)
H_2O-Tb/Eu**1**	<0.1%	0.53 (40%), **0.19** (30%), 0.018 (30%)[b]
		0.51 (24%), 0.20 (76%), −**0.15**[c]
D_2O-Tb/Eu**1**	2%	1.20 (35%), **0.41** (33%), 0.034 (32%)[b]
		1.40 (100%), −**0.29**[c]
Xerogel of Tb/Eu**1**	<0.1%	0.47 (36%), **0.14** (28%), 0.026 (36%)[b]
		0.50 (22%), 0.23 (78%), −**0.081**[c]

[a] λ_{obs} = 450–700 nm. [b] λ_{mon} = 545 nm for Tb. [c] λ_{mon} = 616 nm for Eu. [d] Minus values in lifetimes represent the rise times of luminescence.

recorded using a Shimadzu 3600S UV-VIS-NIR spectrophotometer and a Horiba Jovin-Yvon Fluorolog 3-22 spectrofluorometer, respectively. Luminescence quantum yields and lifetimes were measured by a Hamamatsu 9920-02 absolute photoluminescence quantum yield spectrometer and Quantaurus tau fluorescence lifetime spectrometer, respectively. SEM images were obtained using an Ultra-55 scanning electron microscope (Carl Zeiss AG) equipped with a secondary in-lens electron detector, together with a QUANTAX detector (Bruker Corporation) for EDX. The micro Raman spectra were obtained using Renishow *via* a Reflex spectrometer equipped with a 532 nm diode laser, calibrated to the 520.5 cm^{-1} line of silicon.

Conclusion

Three types of lanthanide ions aggregate to form hydrogels with **1**, even in heavy water. The viscoelastic property of the hydrogel D$_2$O-Tb**1** was identical to that of H$_2$O-Tb**1**, whereas deuterium oxide in the gel D$_2$O-Tb**1** enhanced the efficiency of ff emission of Tb ion. There was no influence on the luminescence of D$_2$O-Eu**1** by heavy water. The fluorescence and phosphorescence bands localized on **1** were observed using D$_2$O-H**1** (metal free; prepared by using hydrochloride) and D$_2$O-Gd**1**, respectively. Raman spectra supported the weak luminescence of Eu in this system. Finally, Eu emission was enhanced in the mixed hydrogel D$_2$O-Tb/Eu**1** through inter-metal energy transfer. These results will provide new aspects for designing hydrogelators in heavy water.

Conflicts of interest

There are no conflicts to declare.

Acknowledgements

References

1 J. L. Kropp and M. W. Windsor, *J. Phys. Chem.*, 1963, **39**, 2769.
2 J. I. Bruce, M. P. Lowe and D. Parker, in *The Chemistry of Contrast Agents in Medical Magnetic Resonance Imaging*, ed. A. E. Merbach and E. Tóth, John Wiley and Sons, 2001, ch 11, p. 437.
3 J. C. Bünzli and C. Piguet, *Chem. Soc. Rev.*, 2005, **34**, 1048.
4 S. V. Eliseeva and J. C. Bünzli, *Chem. Soc. Rev.*, 2010, **39**, 189.

5 J. C. Bünzli, *Chem. Rev.*, 2010, **110**, 2729.
6 L. Prodi, M. Maestri, R. Ziessel and V. Balzani, *Inorg. Chem.*, 1991, **30**, 3798.
7 M. Latva, H. Takalo, V. Mukkala, C. Matachescu, J. C. Rodriguez-Ubis and J. Kankare, *J. Lumin.*, 1997, **75**, 149.
8 K. Miyata, Y. Konno, T. Nakanishi, M. Kobayashi, M. Kato, K. Fushimi and Y. Hasegawa, *Angew. Chem., Int. Ed.*, 2013, **52**, 6413.
9 M. Hatanaka, Y. Hirai, Y. Kitagawa, T. Nakanishi, Y. Hasegawa and K. Morokuma, *Chem. Sci.*, 2017, **8**, 423.
10 S. Sato, A. Ishii, C. Yamada, J. Kim, C. H. Song, A. Fujiwara, M. Takata and M. Hasegawa, *Polym. J.*, 2015, **47**, 195.
11 A. Beeby, I. M. Clarkson, R. S. Dickins, S. Faulkner, D. Parker, L. Royle, A. S. de Sousa, J. A. G. Williams and M. Woods, *J. Chem. Soc., Perkin Trans. 2*, 1999, **3**, 493.
12 R. S. Dickins, D. Parker, A. S. de Sousa and J. A. G. Williams, *Chem. Commun.*, 1996, **6**, 697.
13 S. Ogata, A. Ishii, C. L. Lu, T. Kondo, N. Yajima and M. Hasegawa, *J. Photochem. Photobiol., A*, 2017, **334**, 55.
14 W. D. Horrocks and D. R. Sudnick, *Acc. Chem. Res.*, 1981, **14**, 384.
15 G. Stein and E. Würzberg, *J. Chem. Phys.*, 1975, **62**, 208.
16 S. Ogata, T. Shimizu, T. Ishibashi, Y. Ishiyone, M. Hanami, M. Ito, A. I. S. Kawaguchi, K. Sugimoto and M. Hasegawa, *New J. Chem.*, 2017, **41**, 6385.
17 S. Petoud, S. M. Cohen, J. C. Bünzli and K. N. Raymond, *J. Am. Chem. Soc.*, 2003, **125**, 13324.
18 J. An, C. M. Shade, D. A. Chengelis-Czegan, S. Petoud and N. L. Rosi, *J. Am. Chem. Soc.*, 2011, **133**, 1220.
19 A. R. Hirst, B. Escuder, J. F. Miravet and D. K. Smith, *Angew. Chem., Int. Ed.*, 2008, **47**, 8002.
20 X. Du, J. Zhou, J. Shi and B. Xu, *Chem. Rev.*, 2015, **115**, 13165.
21 K. Nishiyama, Y. Watanabe, K. Watanabe and T. Harada, *Chem. Lett.*, 2012, **41**, 1697.
22 H. Kim and J. Y. Chang, *RSC Adv.*, 2013, **3**, 1774.
23 O. Kotova, R. Daly, C. M. G. dos Santos, M. Boese, P. E. Kruger, J. J. Boland and T. Gunnlaugsson, *Angew. Chem., Int. Ed.*, 2012, **51**, 7208.
24 H. Wang, X. Li, F. Fang and Y. Yang, *Dalton Trans.*, 2010, **39**, 7294.
25 S. Banerjee, R. Kandanelli, S. Bhowmik and U. Maitra, *Soft Matter*, 2011, **7**, 8207.
26 M. Li, Y. Wang, Y. Chen and S. A. Zhang, *Photochem. Photobiol. Sci.*, 2014, **13**, 1025.
27 T. Wang, P. Li and H. Li, *ACS Appl. Mater. Interfaces*, 2014, **6**, 12915.
28 G. M. Peters, L. P. Skala and J. T. Davis, *J. Am. Chem. Soc.*, 2016, **138**, 134.
29 M. Yamanaka, K. Yanai, Y. Zama, J. Tsuchiyagaito, M. Yoshida, A. Ishii and M. Hasegawa, *Chem.–Asian J.*, 2015, **10**, 1299.
30 J. Takeshita, Y. Hasegawa, K. Yanai, A. Yamamoto, A. Ishii, M. Hasegawa and M. Yamanaka, *Chem.–Asian J.*, 2017, **12**, 2029.
31 Z. Li, L. E. Z. Buerkle, M. R. Orseno, K. A. Streletzky, S. Seifert, M. A. Jamieson and S. J. Rowan, *Langmuir*, 2009, **26**, 10093.

32 D. W. Horrocks and D. R. A. Sudnick, *J. Am. Chem. Soc.*, 1979, **101**, 334.

33 R. M. Supkowski and W. D. Horrocks, *Inorg. Chim. Acta*, 2002, **340**, 44.

34 M. Li and P. R. Selvin, *J. Am. Chem. Soc.*, 1995, **117**, 8132.

35 M. Kawa and J. M. Fréchet, *Chem. Mater.*, 1998, **10**, 286.

36 A. Sillen and Y. Engelborghs, *J. Photochem. Photobiol., A*, 1998, **67**, 475.

37 M. Hasegawa, H. Ohtsu, D. Kodama, T. Kasai, S. Sakurai, A. Ishii and K. Suzuki, *New J. Chem.*, 2014, **38**, 1225.

38 K. Binnemans, *Coord. Chem. Rev.*, 2015, **295**, 1.

39 P. R. Matthes, C. J. Höller, M. Mai, J. Heck, S. J. Sedlmaier, S. Schmiechen, C. Feldmann, W. Schnick and K. Müller-Buschbaum, *J. Mater. Chem.*, 2012, **22**, 10179.

40 S. Katagiri, Y. Hasegawa, Y. Wada and S. Yanagida, *Chem. Lett.*, 2011, **33**, 1438.